Accident Analysis and Prevention 128 (2019) 230–239

Contents lists available at ScienceDirect

Accident Analysis and Prevention

journal homepage: www.elsevier.com/locate/aap

A vehicle speed harmonization strategy for minimizing inter-vehicle crash risks

Hyunjin Park[a], Cheol Oh[b,*]

[a] Transportation Research Division, Korea Expressway Corporation Institute, 208-96, Dongbu-daero 922beon-gil, Dongtan-myeon, Hwaseong-si, Gyeonggi-do 18489, Republic of Korea

[b] Department of Transportation and Logistics Engineering, Hanyang University Erica Campus, 55 Hanyangdaehak-ro, Sangnok-gu, Ansan 15588, Republic of Korea

ARTICLE INFO

Keywords:
Risk estimation
Speed control
Risk map
Risk minimization
Vehicle trajectory data

ABSTRACT

Recent technological advancements have facilitated the implementation of speed harmonization based on connected and automated vehicles (CAV) to prevent crashes on the road. In addition, trajectory-level vehicle controls are receiving substantial attention as sensors, wireless communications, and control systems are rapidly advancing. This study proposes a novel vehicle speed control strategy to minimize inter-vehicle crash risks in automated driving environments. The proposed methodology consists of the following three components: a risk estimation module, a risk map construction module, and a vehicle speed control module. The essence of the proposed strategy is to adjust the subject vehicle speed based on an analysis of the interactions among a subject vehicle and the surrounding vehicles. Crash risks are quantified by a fault tree analysis (FTA) method to integrate the crash occurrence potential and crash severity at every time step. A crash risk map is then constructed by projecting the integrated risk of the subject vehicle into a two-dimensional space composed of relative speed and relative spacing data. Next, the vehicle speed is continuously controlled to reach the target speed using risk map analysis to prevent a crash. The performance of the proposed methodology is evaluated by a VISSIM simulator with various traffic congestion levels and market penetration rates (MPR) of controlled vehicles. For example, an approximate 50% reduction rate of the crash potential was achievable without a loss of the operational performance of the traffic stream when all vehicles were controlled by the proposed methodology under the level of service (LOS) C conditions. This study is meaningful in that vehicle speed control is performed for the purpose of speed harmonization in a traffic stream based on a comprehensive analysis of inter-vehicle risks. It is expected that the outcome of this study will be valuable for supporting the development of vehicle control systems for preventing crashes in automated driving environments.

1. Introduction

Traffic safety is a top priority issue to be addressed in the transportation field because it is directly related to human lives. Among the various countermeasures employed to prevent crashes on the road, advanced vehicular technologies have attracted much attention for the reduction of crashes resulting from human driver errors. In particular, speed harmonization based on controlling the vehicle speed is a promising measure to enhance the safety performance of the traffic steam by preventing crashes in automated driving environments.

For effective speed harmonization, individual vehicle maneuvering should be properly controlled by connected and automated vehicle (CAV) technology. Automated vehicle speed controls have recently been implemented by several commercialized vehicular technologies, including adaptive cruise control (ACC), cooperative adaptive cruise control (CACC), and the automatic emergency braking system (AEBS). It has been widely reported that such longitudinal vehicle control measures can improve traffic flow stability representing the indirect crash potential (Shrivastava and Li, 2000; Darbha and Rajagopal, 1999; Schakel et al., 2010; Pueboobpaphan and Arem, 2011; Jeong et al., 2017). These systems are intended to maintain the proper spacing between the leading and following vehicles. Recently, research on vehicle control and safety has been conducted in relation to autonomous vehicles. These studies include the identification of risks on the road (Kim et al., 2017), the planning of routes to avoid obstacles (Ji et al., 2017) and the use of vehicle controls considering driver comfort (Pan et al., 2017). It has also been demonstrated based on extensive simulations that environmental impacts can be reduced by CAVs, which can also provide safety and delay improvements (Talebpour et al., 2013; Wang et al., 2015; Li et al., 2014).

* Corresponding author.
E-mail addresses: snowboard@ex.co.kr (H. Park), cheolo@hanyang.ac.kr (C. Oh).

https://doi.org/10.1016/j.aap.2019.04.014
Received 4 January 2019; Received in revised form 5 March 2019; Accepted 17 April 2019
Available online 06 May 2019
0001-4575/

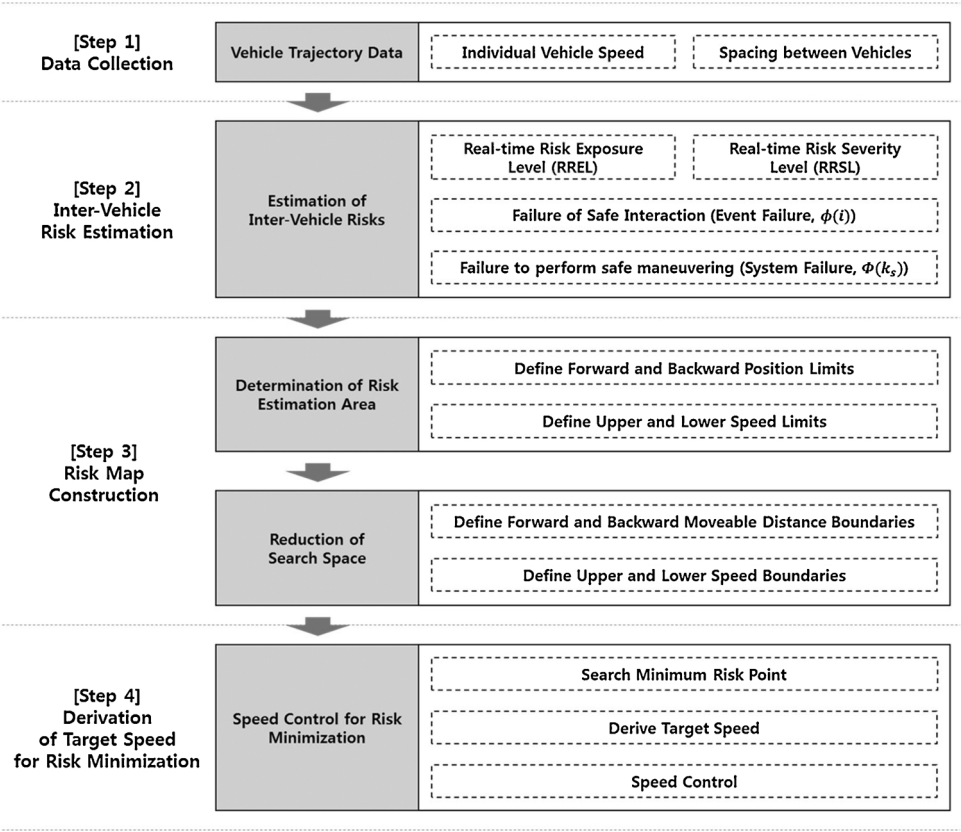

Fig. 1. Overall framework.

In addition to studies on longitudinal vehicle control systems, research on lateral vehicle maneuvering has also been actively conducted. For example, Jula et al. (2000) performed a study to determine the minimum lateral spacing for safe lane changes. Additionally, Schubert et al. (2010) evaluated the safety of lane changes by a Bayesian network technique using vehicle sensors. Xiaorui and Hongxu (2013) proposed a lane change model integrated with a car-following model. Recent interest on autonomous vehicles has led to research on lane change decision assistance systems (LCDAS). Shiller et al. (2008) attempted to prevent crashes while a vehicle performs a lane change by providing warning information. Schmidt et al. (2014) defined various lane change behaviors collected from actual driving trajectories and developed a reliable lane change prediction model. Wang and Stamatiadis (2013, 2014) conducted a study to derive surrogate safety measures (SSM) that could evaluate the safety of lane change events. Most of the studies discussed above dealt with methods on how to successfully support safe lane changes and effectiveness evaluations.

It is expected that we provide a valuable opportunity to control the vehicle speed based on the recognition of the driving situation of the surrounding vehicles in automated driving environments. To date, we are not aware of any study that analyzed comprehensive crash risks resulting from individual vehicle interactions and or the adjustment of vehicle speeds toward the minimization of crash risks. Therefore, a novel method needs to be devised to fully facilitate the benefits of automated driving environments that enable us to identify the position and speed of surrounding vehicles. This has motivated our study. Vehicle speed control consists of two stages in automated driving environments. In the upper level, a decision should be made to select the acceleration of the vehicle. In the lower level, the throttle and braking operations of the vehicle are performed. This study focuses on the upper level, which can be regarded as a strategic development.

The proposed methodology consists of three components. The first is to identify inter-vehicle crash risks by incorporating the crash occurrence potential and crash severity based on a fault tree analysis technique (FTA), which results from vehicle interactions between the subject and surrounding vehicles. The second is to construct a risk map. Once the subject vehicle identifies crash risks, the algorithm projects the integrated risk of the subject vehicle into a space composed of two dimensions, namely, the relative speed and spacing, where the subject vehicle can physically exist. Lastly, the proposed algorithm calculates a target speed to minimize crash risks on the risk map and adjust the vehicle speed to follow target values obtained at every time step. The VISSIM microscopic traffic simulator was used to implement the proposed methodology in real-time simulation environments. The applied programming interface (API) technique was used to code our methodology and to plug it into VISSIM to investigate how it works in terms of both safety and operational performances.

The remainder of this paper is organized as follows. Section 2 presents the proposed methodology, including an overall evaluation framework composed of risk estimation, risk map construction, and target speed identification. Section 3 presents the analysis results along with a discussion. Finally, Section 4 presents the summary and conclusions of this study and possible future research directions based on the identified limitations of this study.

2. Methodology

2.1. Overall framework

This study attempts to develop a method for vehicle speed control based on the minimization of the inter-vehicle crash potential in an automated driving environment. It is assumed that the speeds and positions of a subject and the surrounding vehicles are available from vehicle sensors. The proposed methodology continuously estimates real-time crash potentials resulting from the interactions among the subject vehicle and surrounding vehicles and identifies a target speed

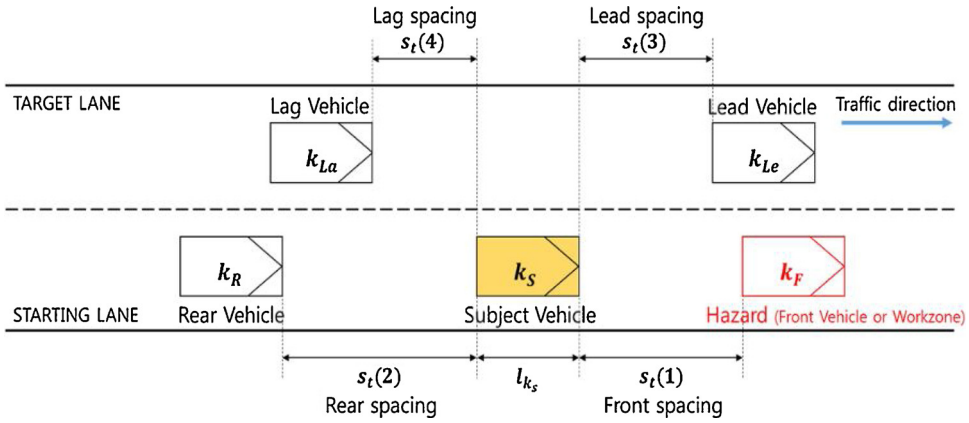

Fig. 2. Definitions of the subject vehicle and surrounding vehicles.

value leading to the minimum inter-vehicle crash potential at every time step. The overall procedure for the vehicle speed control consisting of four steps is presented in Fig. 1. More details on each step are presented in the following sections.

2.2. Inter-vehicle risk estimation

The first step of the proposed methodology is to collect individual vehicle trajectory data, including vehicle positions and speeds. The interacting vehicles to be analyzed differ according to the movement of the subject vehicle. When the subject vehicle simply performs car-following, k_F and k_R are regarded as the interaction vehicles. Meanwhile, when the subject vehicle changes lanes, k_{Le} and k_{La} should be further taken into consideration when estimating the risk in addition to k_F and k_R. Here, we describe how to estimate the risk and construct the risk map for the lane change case, which is more complex than the car-following case. A total of four adjacent vehicles affect the risk of an accident when a subject vehicle (k_S) travels on a two-lane road, as shown in Fig. 2. The four adjacent vehicles include the front (k_F) and rear (k_R) vehicles in the traveling lane and the leading (k_{Le}) and lagging (k_{La}) vehicles in the adjacent lane.

The second step is to estimate the real-time crash risks based on a fault tree analysis (FTA) integrating the real-time risk exposure level (RREL) and real-time risk severity level (RRSL), as shown in Fig. 3. Four interaction events with adjacent vehicles (k_F, k_R, k_{Le}, *and* k_{La}) are evaluated in terms of the crash potential based on the RREL and RRSL. The event failure of the proposed FTA analysis is defined as the failure of safe vehicle interaction between a subject vehicle and the surrounding vehicles denoted by (i). The failure of safe vehicle interaction between the subject vehicle and adjacent vehicles (k_F, k_R, k_{Le}, and k_{La}) is denoted by $\varphi(1)$, $\varphi(2)$, $\varphi(3)$, and $\varphi(4)$, respectively. As shown in Eq. (1), the fault of event $\varphi(i)$ is calculated based on a combination of failure factors, including the RREL and RRSL. Then, the integration of $\varphi(i)$ is conducted to estimate the risk level represented by a probabilistic measure of $k_S$failing to perform a safe maneuvering ($\Phi(k_s)$) as shown in Eq. (2).

To derive the RREL, which is a surrogate safety measure to represent the rear-end crash potential, the time remaining until the stopping distance index (SDI) becomes zero (TSO) is calculated. The TSO is the time remaining until the vehicle enters a state where it is impossible to avoid a dangerous situation ahead. The calculated TSO is applied to the exponential decay function (EDF) to calculate the probability of the occurrence of an accident from 0 to 1. To determine the RRSL, the time to collision with deceleration condition (TTCD), which is defined as the time remaining between the current time t when the vehicles start braking and the time when the spacing of two vehicles becomes zero, is calculated. Then, the TTCD is further used to obtain Delta V, which is the difference in speed at the moment ($\hat{V}$) when the subject vehicle

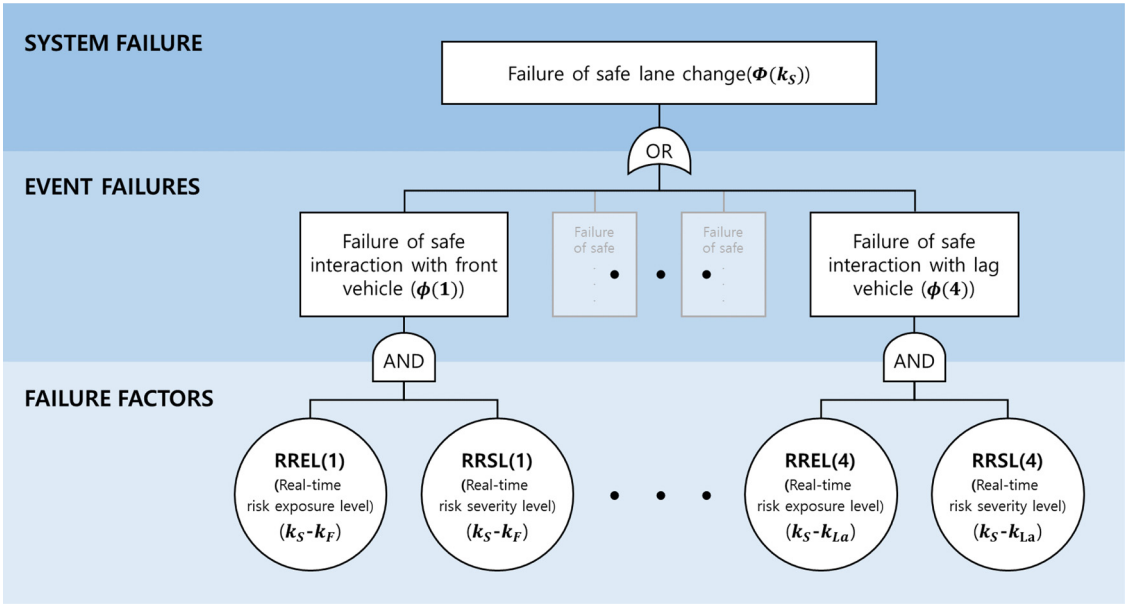

Fig. 3. Fault tree structure of failure to perform safe lane change (Park et al., 2018).

collides with the interacting vehicle. Utilizing the actual observed *Delta V* and the theoretically observable maximum velocity difference ($Delta\ V_{MAZ}^{obs}$), the RRSL is expressed as a probabilistic measure between 0 and 1. More details on the risk estimation method of deriving the risk exposure level and the risk severity level are presented in the literature (Park et al., 2018).

$$\varphi(i) = RREL(i) \times RRSL(i) \tag{1}$$

where φ: event failure (failure of safe vehicle interaction)
RREL: real-time risk exposure level
RRSL: real-time risk severity level

$$\Phi(k_s) = 1 - \prod_{i=1}^{4} [1 - \varphi(i)] \tag{2}$$

where Φ: system failure (probability of failure to perform safe maneuvering)
φ: event failure
k_s: subject vehicle

2.3. Risk map construction

2.3.1. Concept of risk map

The risk map consists of time-varying contour lines indicating the risks of the subject vehicle. The risk map can be constructed by projecting the estimated risk values into a two-dimensional plane composed of the relative speed and spacing. The risk is estimated for the potentially available plane at the next time step at the current vehicle position and speed. The origin points of the risk map (0,0) represents the current speed and position of the subject vehicle. As shown in Fig. 4(a), the relative position and the relative speed of the surrounding vehicles that interact with the subject vehicle can be expressed in a risk map. The vehicles located in front of the subject vehicle (k_F and k_{Le}) are plotted on the right with respect to the y-axis. Conversely, the vehicles located behind the subject vehicle (k_R and k_{La}) are plotted on the left. Vehicles faster than the subject vehicle are located above the x-axis, and slower vehicles are located below the x-axis. The risk increases when the vehicle spacing becomes shorter and when the speed of the rear vehicle is faster than the speed of the preceding vehicle.

2.3.2. Determination of the risk estimation area

To establish the risk estimation area of the subject vehicle, the upper and lower limits for the relative speed and position are determined. Regarding the boundaries for the relative position, the maximum distance that can be detected by the vehicle sensor is set as a boundary. These boundaries are referred to as the forward and backward position limits, which are $FL_k^{\Delta p}(t)$ and $BL_k^{\Delta p}(t)$ in this study, respectively. Regarding the relative speed, the relative maximum and minimum speeds that can be observed from the current speed of the subject vehicle are selected as boundaries, which are referred to as the upper and lower speed limits, such as $UL_k^{\Delta v}(t)$ and $LL_k^{\Delta v}(t)$, respectively. The four aforementioned boundaries constitute 4 quadrants in Fig. 4(b). Therefore, the proposed algorithm searches for the minimum risk point only within the shaded area.

2.3.3. Search space reduction

Next, the proposed method increases the efficiency of the speed control algorithm by eliminating logically and physically inaccessible areas on the risk map; this process is referred to as search space reduction in this study. First, the physical constraint is for taking relative positions into consideration. In this study, the maximum position where the subject vehicle can move forward or backward is set as the physical constraint condition of the subject vehicle. The subject vehicle can be moved between the front and the rear vehicle within the traveling lane. Additionally, the subject vehicle can be located between the lead and the lag vehicle on the target lane while changing lanes. Therefore, the farthest position at which the subject vehicle can move forward, which is defined as the forward moveable distance boundary ($FB_k^{\Delta p}(t)$), is determined as a minimum value among the relative positions of k_F and k_{Le} as shown in Fig. 4(c). Likewise, the farthest position at which the subject vehicle can move backward, which is defined as the backward moveable distance boundary ($BB_k^{\Delta p}(t)$), is determined as a maximum value among the relative positions of k_R and k_{La}. Second, the logical constraint is determined for taking relative speeds into consideration. It is necessary to consider the speed harmonization with surrounding interaction vehicles because the ultimate purpose of the proposed speed control method is to minimize the crash risk by adjusting vehicle speeds. From this perspective, the maximum and minimum driving speeds are set as logical constraints, which are the upper and lower target speed boundaries denoted as $UB_k^{\Delta v}(t)$ and $LB_k^{\Delta v}(t)$, respectively. When there is no interaction vehicle, the risk is estimated up to the risk estimation area limited in the previous step above.

2.4. Derivation of the target speed for risk minimization

The risk map developed in this study is a two-dimensional plane representation of the risk by the position and speed of the subject vehicle, which can be defined by Eq. (3). If all of the relative positions x and relative speeds y that can be potentially occupied by the subject vehicle are defined as the elements of a constrain condition C, then the risk map is composed of all of the risk values. If all of the virtual relative positions x and relative velocities y that can be changed by the subject vehicle are defined as the elements of the constraint condition C, all of the risk values calculated as x and y according to the condition are expressed as a risk map. Here, the constraint C represents the search space reduction process for creating a risk map in the previous section as expressed by Eq. (4). c_1 is the performance of the sensor capable of observing both the front and the rear, and c_2 is the observable speed range of the vehicle. c_3 and c_4 are the areas considering the speed and position of the surrounding vehicles that interact with the subject vehicle.

$$\forall\ (x,\ y) \in C,\ \Phi_t^{(x,y)} \Rightarrow Riskmap_k(t) \tag{3}$$

$$C = \{(x,\ y)c_1 \wedge c_2 \wedge c_3 \wedge c_4\} \tag{4}$$

where,

$$c_1 : sensor\ capability(backward) \le x \le sensor\ capability(forward)$$

$$c_2 : 0km/h \le y \le 300km/h$$

$$c_3 : [\max(FL_k^{\Delta p}(t),\ FB_k^{\Delta p}(t))] \le x \le [\min(BL_k^{\Delta p}(t),\ BB_k^{\Delta p}(t))]$$

$$c_4 : [\min(UL_k^{\Delta s}(t),\ LB_k^{\Delta s}(t))] \le y \le [\max(UL_k^{\Delta s}(t),\ LB_k^{\Delta s}(t))]$$

This study established an optimization problem that minimizes the risk resulting from the interactions among the subject vehicle and surrounding vehicles in order to derive the target speed at every time step. The principle of the proposed method is to control the vehicle speed based on the identification of the relative speed and position that can minimize the crash risk under the given constraints discussed previously. This problem is expressed in Eq. (5). First, the relative speed $\tilde{y}$, which minimizes the risk of the vehicle k, is obtained from the risk map. Then, the target speed $\tilde{v}_k(t)$ of the vehicle k at time t can be determined by the current traveling speed $v_k(t)$ and the relative speed $\tilde{y}$ as shown in Eq. (6).

$$\tilde{y} = \underset{y}{\operatorname{argmin}}\ Riskmap_k(t) \tag{5}$$

where

$\tilde{y}$: *the relative speed to minimize the crash risk*

$$\tilde{v}_k(t) = v_k(t) + \tilde{y} \tag{6}$$

where

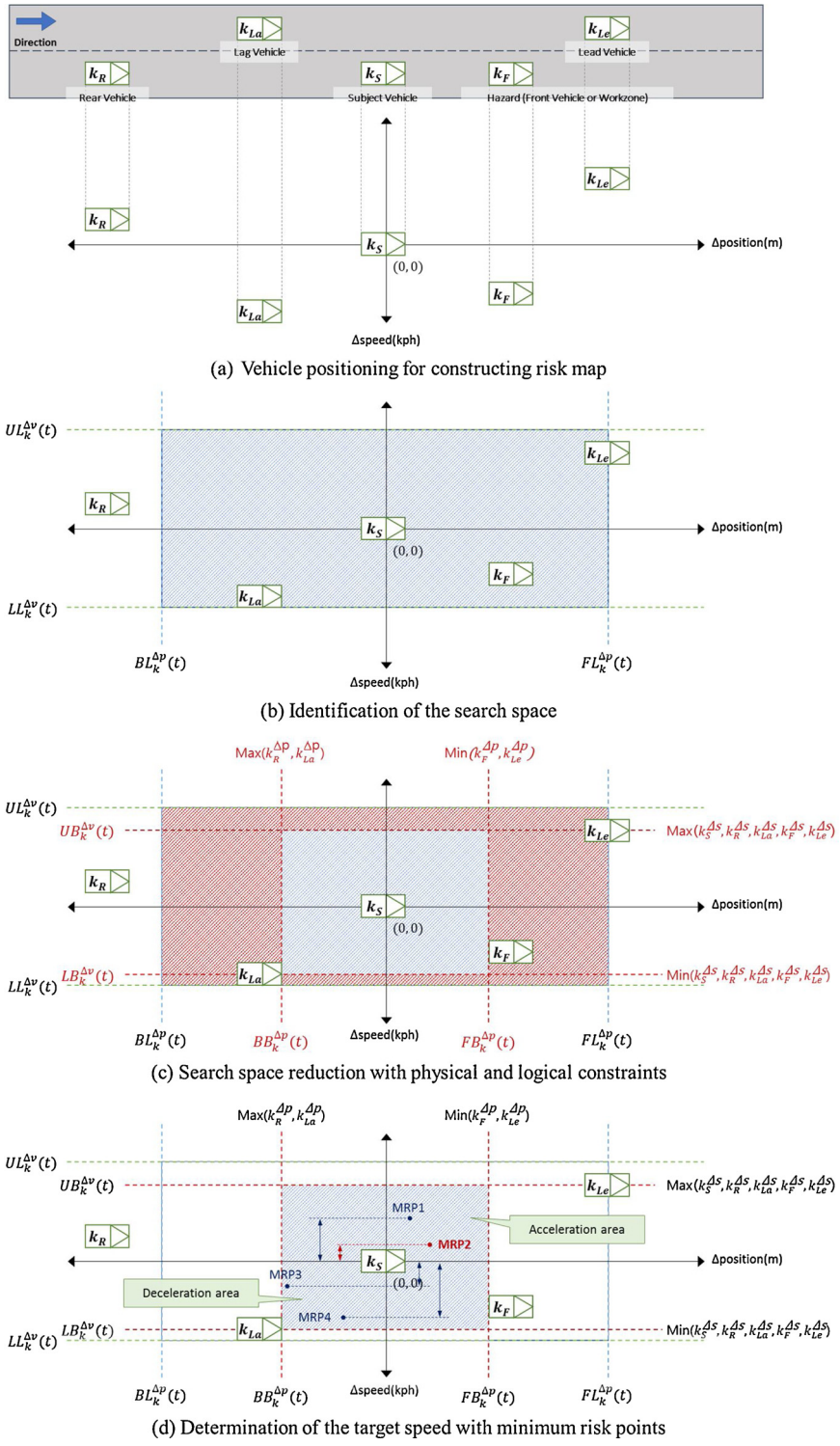

(a) Vehicle positioning for constructing risk map

(b) Identification of the search space

(c) Search space reduction with physical and logical constraints

(d) Determination of the target speed with minimum risk points

Fig. 4. Risk map construction.

$v_k(t)$: *travel speed of vehicle k at time step t*

$\tilde{v}_k(t)$: *target speed of vehicle k at time step t*

The risk map presented in this study is based on the relative speed and relative distance between the subject vehicle and the surrounding interactive vehicles. Therefore, the relative distance may be reduced in case the speed of interacting vehicle approaching from the rear is faster than that of the subject vehicle. For this reason, we need to consider minimum risk points in upper-left and lower-right regions.

The proposed speed control algorithm is presented in Fig. 5. First, the position and speed information of the subject vehicle and the surrounding vehicles are collected, and a risk map is created. If the case is such that the risk of the subject vehicle estimated at the present time is equal to or less than the minimum risk value on the risk map, speed control is not performed. On the other hand, if the speed of the subject vehicle is greater than the minimum risk value, the vehicle is dynamically controlled at a target speed that minimizes the risk.

The risk of the subject vehicle can be reduced by controlling the

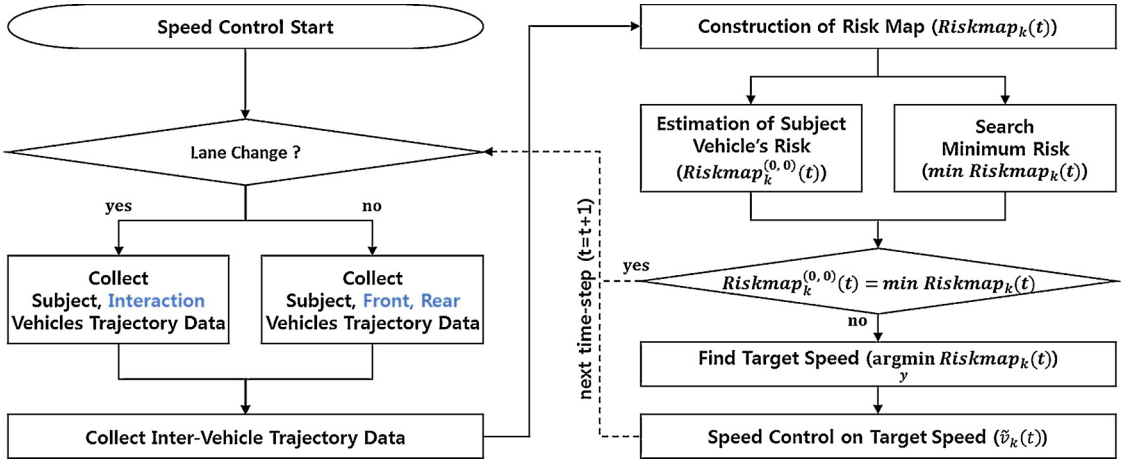

Fig. 5. Speed control algorithm.

speed based on a relative speed point corresponding to the minimum risk value on the risk map. When multiple minimum risk values are observed in the risk map, as shown in Fig. 4(d), the vehicle speed is controlled to the point where the change in the relative speed is minimal. This is because it is preferable to adjust the speed so that the change of the acceleration of the vehicle is minimized.

3. Simulation analysis

3.1. Simulation environments

To demonstrate the feasibility of this study, a VISSIM microscopic traffic flow simulation program was used in this study. As shown in Fig. 6, A two-lane freeway segment near the Gonjiam interchange (IC) on the Jungbu Expressway in Korea was simulated. The study area was a freeway mainline segment, and one lane was blocked due to a work zone. The analysis was carried out considering that the impact of the work zone reached to 2 km upstream of the work zone. The speed limit is 110 kph, and the capacity is approximately 2100 passenger cars per hour per lane (pcphpl). A simulation network was constructed by using image data taken by a drone. As shown in Fig. 7, a total of 265 vehicle trajectories (201 passenger cars, 61 trucks, 3 buses) were collected from the images taken by a drone. Average speed and lane change position information were then extracted by vehicle type to make sure that simulated vehicles move as closely as possible to the actual field situation. This effort can be regarded as a simplified simulation calibration although more in-depth investigations should be needed with a larger dataset. We analyzed five scenarios (A–E) of the highway level of service (LOS) by applying the methodology presented in this research. A sixth (F) LOS scenario was not analyzed because dangerous situations representing a high crash severity were not readily observable due to low vehicle speeds under congested traffic conditions. The analysis time for a simulation was set to 15 min, and the warm-up period was set to 15 min. Relevant previous studies using VISSIM in the literature have used the average value of simulation results calculated by repeating 10 times or so. (Jeong and Oh, 2017; Park et al., 2018; Lee et al., 2019). In the same way as in the previous studies, simulations of five scenarios were repeated 10 times and the average values were computed for the scenarios. The results of VISSIM analysis did not change significantly with each iteration.

Fig. 8 shows the overall process for implementing the proposed vehicle speed control algorithm, which was coded using a Com-interface within the VISSIM simulation environment. After the warm-up period, we selected the scenarios for analysis and collected all of the vehicle speed and location data at every time-step. Once a risk map for a subject vehicle was constructed, vehicle speed control was performed to minimize the crash risk. When a series of processes was completed, a new scenario was set up, and the simulation analysis was repeated. If speed control was performed without considering the performance of the vehicle, abnormal maneuvering behaviors would be observed. We

Fig. 6. A snapshot of the Jungbu Expressway, captured by a drone.

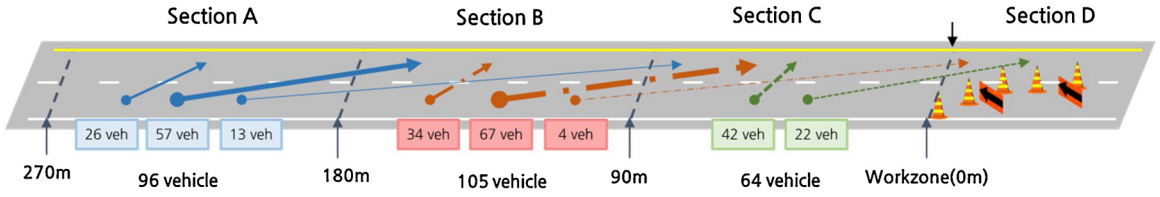

Section	From	A			B			C		Total (veh)	Avg. Speed(kph)	
	To	A	B	C	B	C	D	C	D		Field	Simulation
Passenger cars		20	42	6	26	31	3	33	17	201	99.8	105.8
Trucks		6	14	2	8	16	1	9	5	61	79.1	84.1
Buses			1	1		1				3	83.9	79.2
Total(veh)		26	57	13	34	67	4	42	22	265	94.8	98.1

Fig. 7. Lane change patterns and average speeds collected by a drone.

implemented the speed control in the simulation environment using the desired speed parameter offered by VISSIM. The use of a desired speed parameter is the most effective method to implement the proposed methodology within the simulation because the vehicle speed is changed at the desired speed considering the performance of the vehicle.

3.2. Results

The risk map of a subject vehicle is constructed at every time step, and the target speed is derived to minimize the crash risk of the subject vehicle based on the analysis of the vehicle interactions. Then, the vehicle speed is controlled toward a target speed by the proposed algorithm shown in Fig. 5.

Fig. 9 illustrates a risk map as an example using all of the relative speeds and relative positions within the constraint conditions of a subject vehicle using the simulation data. This vehicle is located at the coordinates (0, 0), and the interaction vehicles, namely, the front, rear, lead, and lag vehicles, are located at (87.85, -10.72), (-50.03, -0.81), (50.66, 4.28), and (38.64, 9.37), respectively. The risk minimum point (RMP) was derived from the coordinates (-35.75, 7.82). Therefore, the target speed at this time step was determined to be 113.54 kph, which is

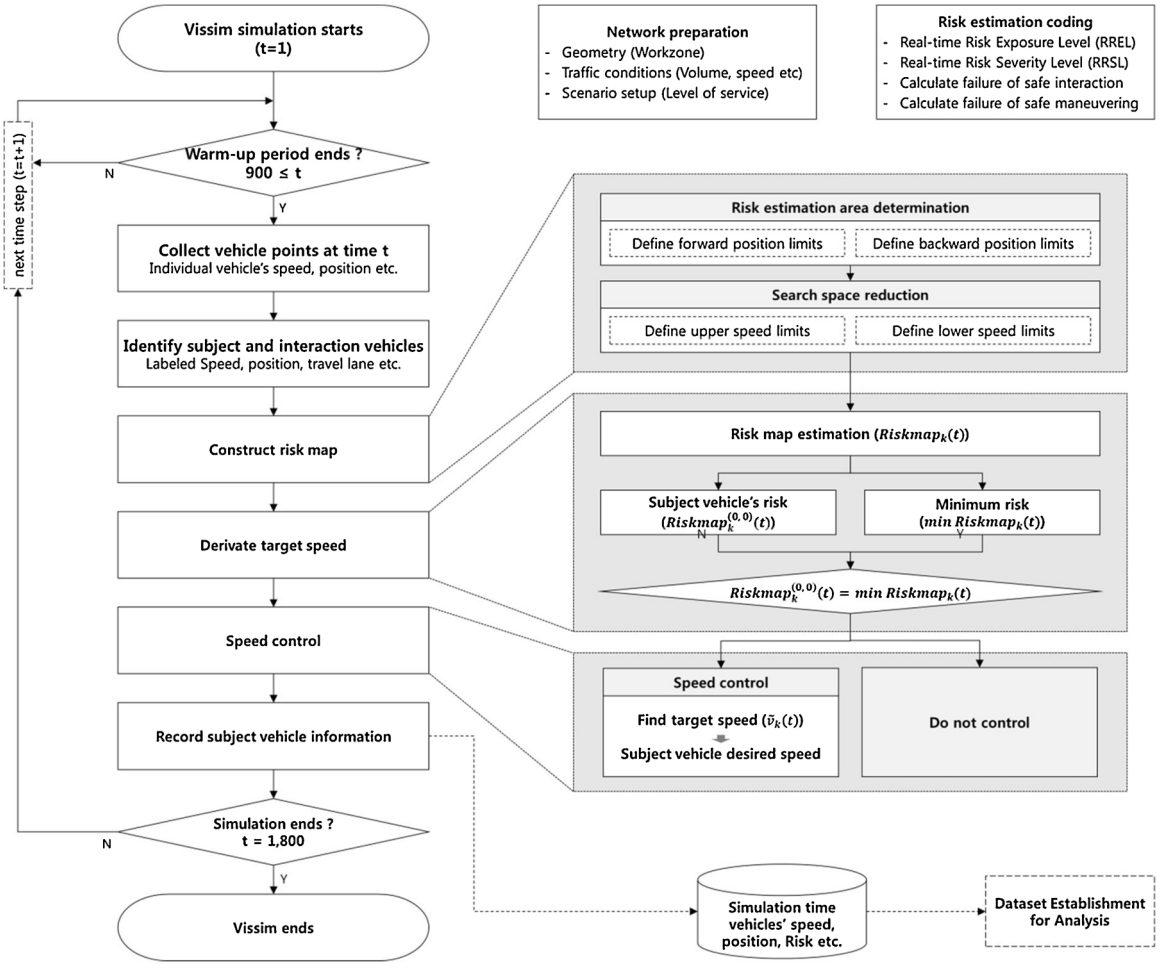

Fig. 8. Implementation of proposed methodology with VISSM.

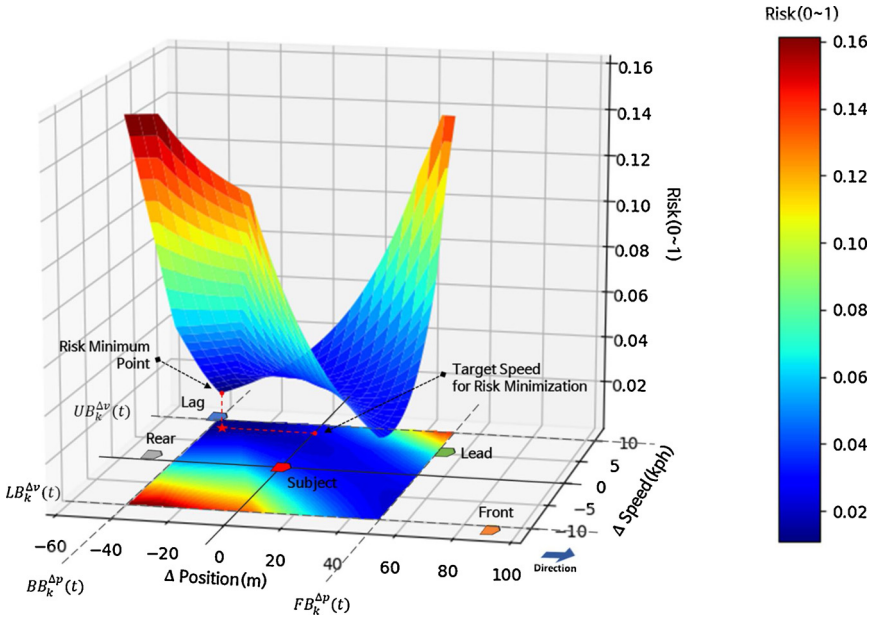

Fig. 9. Example of the risk map and target speed.

5 kph added to the current speed of 105.72 kph.

The changes in the vehicle trajectory and risk profile when the speed control process is both performed and not performed during the simulation are compared in Fig. 10. Fig. 10(a) shows a result of the speed control, and Fig. 10(b) shows a case resulting from the speed control of the subject vehicle. A section of construction is installed at 1640 m on the simulation road network. The subject vehicle traveling in the right lane changes lanes from the right to the left at the front of the construction zone. In the case where speed control is not performed, the subject vehicle attempted to change lanes in front of the construction area ahead in Section A. However, the risk increased, and the vehicle could not change lanes due to the rapidly approaching lag vehicle. Although the subject vehicle slowed down to change lanes, the risk increased because the spacing between the subject vehicle and the lag vehicle and the spacing between the subject vehicle and the construction zone were both getting smaller in Section B. Thereafter, the subject vehicle changed the lane after the lag vehicle had passed. The risk in Section C then decreased after completing the lane change. Meanwhile, the proposed speed control algorithm made the subject vehicle speed up based on the identification of a target speed higher

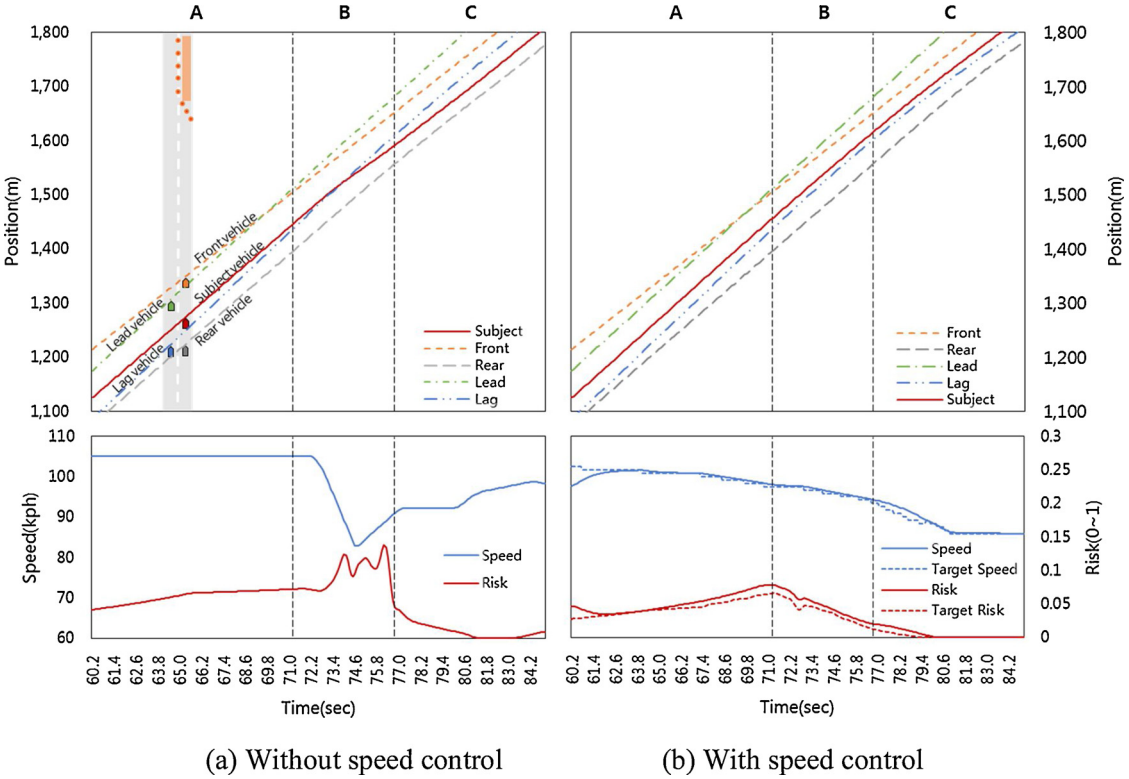

Fig. 10. Example of risk and speed profiles.
(a) Without speed control (b) With speed control.

Risk(0~1)		Controlled Vehicle Market Percent Rate (%)										
		0	10	20	30	40	50	60	70	80	90	100
Level of Service (Vol)	A (1200)	0.0363 (0.0%)	0.0335 (-7.8%)	0.0314 (-13.5%)	0.0302 (-16.9%)	0.0267 (-26.5%)	0.0237 (-34.8%)	0.0204 (-43.7%)	0.0196 (-45.9%)	0.0152 (-58.2%)	0.0120 (-67.1%)	0.0058 (-84.0%)
	B (1800)	0.1165 (0.0%)	0.0957 (-17.8%)	0.0828 (-28.9%)	0.0777 (-33.3%)	0.0780 (-33.0%)	0.0715 (-38.6%)	0.0699 (-40.0%)	0.0523 (-55.1%)	0.0466 (-60.0%)	0.0441 (-62.2%)	0.0196 (-83.2%)
	C (2400)	0.1031 (0.0%)	0.0978 (-5.1%)	0.0978 (-5.1%)	0.0881 (-14.6%)	0.0923 (-10.4%)	0.0867 (-15.9%)	0.0812 (-21.2%)	0.0796 (-22.7%)	0.0734 (-28.8%)	0.0680 (-34.0%)	0.0510 (-50.5%)
	D (3500)	0.0924 (0.0%)	0.0973 (5.3%)	0.0883 (-4.4%)	0.0868 (-6.1%)	0.0858 (-7.2%)	0.0837 (-9.4%)	0.0815 (-11.8%)	0.0820 (-11.2%)	0.0793 (-14.2%)	0.0762 (-17.5%)	0.0755 (-18.3%)
	E (4400)	0.0953 (0.0%)	0.0937 (-1.7%)	0.0923 (-3.1%)	0.0891 (-6.5%)	0.0909 (-4.6%)	0.0861 (-9.7%)	0.0836 (-12.3%)	0.0842 (-11.7%)	0.0853 (-10.5%)	0.0868 (-9.0%)	0.0808 (-15.2%)

*Risk(Ratio)

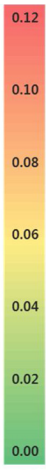

Fig. 11. Risk patterns according to different LOS and MPR levels.

than the current speed. Therefore, the subject vehicle gradually accelerated. As a result, the risk was lower than when no speed control was applied. This result implied that the driving safety was improved from the viewpoint of speed harmonization, because the magnitude of the speed change was not large. Finally, the subject vehicle changed the route to the front of the lag vehicle for the lane change in the speed control case, while the subject vehicle without speed control performed a lane change to the rear of the lag vehicle.

Two examples of the movements of individual cars and the changes in the risk by speed control were examined above. Next, a collective analysis was conducted to investigate the overall effectiveness of speed control. The average risk values and the rates of change in the risks during different levels of the traffic volume and market penetration rate (MPR) of controlled vehicles were presented in Fig. 11. As the traffic volume increases, the average risk of individual vehicles tends to increase. Meanwhile, the average risk of individual vehicles decreases as the MPR of controlled vehicles increases. Compared with the case of 0% MPR, which represents the absence of speed control, the reduction in the average risk was considerably large under LOS A conditions. For example, if 40% of vehicles are controlled by the proposed method under LOS A, it is expected to reduce the crash potential by approximately 26%. In addition, the average risk decreased as the MPR increased. For example, an approximate reduction rate of 50% of the crash potential was achievable when the MPR reached 100% under LOS C conditions, compared with the case of 0% MPR. Therefore, the proposed speed control method is effective for the enhancement of traffic safety by reducing crash potentials.

Another important issue in traffic safety analysis is the need to assess the operational performance of traffic streams, because countermeasures to enhance the safety would reduce the operational efficiency that can be represented by the travel speed. To investigate the effect of the proposed speed control method on changes in the travel speed, the average travel speed and the rates of change in the speeds were analyzed, as shown in Fig. 12. A risk analysis of the case was also completed. As the traffic volume increased, the average speed tended to decrease. The average speed tended to decrease slightly as the MPR gradually increased. However, the operational performance was improved at higher MPR levels under relatively heavy traffic conditions such as LOS C, D and E. As a result, it can be said that the substantial benefits of the safety enhancement are obtained without a significant loss of the operational performance.

4. Conclusions

Recent advances in advanced vehicular technologies with regard to automated driving environments have facilitated the development of various sophisticated strategies and methodologies for controlling vehicles to prevent crashes on the road. This study developed a novel methodology for vehicle speed control while integrating the previously developed risk estimation method to minimize inter-vehicle risks. A valuable feature of the proposed method is the construction of a two-dimensional risk map based on the analysis of interactions between a subject vehicle and surrounding vehicles. Then, the vehicle speed is continuously controlled to reach the target speed, which is obtained through risk map analysis, in order to prevent a crash.

The feasibility of the proposed control method was demonstrated by microscopic simulation experiments. The speed control algorithm developed in this study was coded using a Com-interface plugged into the VISSIM simulation environment. Various LOS conditions and MPR levels, which were expected to affect the effectiveness of the algorithm, were taken into consideration while conducting the simulation analyses. Promising test results showed that meaningful safety benefits were achievable without a reduction in the operational performance. It is expected that the outcome of this study would effectively support the development of vehicle control systems for preventing crashes in automated driving environments.

Promising further applications of the proposed methodology are as follows. First, safer lateral maneuvering of autonomous vehicles can be supported by the proposed method that attempts to achieve the speed harmonization with adjacent vehicles. Second, in-vehicle warning information, which leads to effective avoidance maneuver, can be delivered to drivers in a hazardous situation where the crash potential is observed above a certain threshold. It can be said that the first application is for the autonomous vehicle, while the second is for the manually driven vehicle. Third, the outcome of this study would be valuable in evaluating the effectiveness of various ADAS technologies in terms of obtainable safety benefits because the method developed in the study is able to quantify the comprehensive crash potential. Lastly, in addition to the vehicle safety, the traffic stream safety can be measured by proper spatio-temporal aggregations of the crash potential of individual vehicles.

Although useful insights were derived from this study, further research needs to be conducted to achieve results with greater reliability. First, there is an opportunity to improve the risk estimation method. Various contributing factors affecting inter-vehicle risks need to be considered when estimating the risk, including adverse weather and road geometric conditions in addition to the vehicle performance. Second, more effective and intelligent techniques for obtaining the target speed should be studied. For example, machine learning techniques that have received much attention recently should be applied

Speed(kph)		Controlled Vehicle Market Percent Rate (%)										
		0	10	20	30	40	50	60	70	80	90	100
Level of Service (Vol)	A (1200)	108.02 (0.0%)	105.94 (-1.9%)	104.39 (-3.4%)	102.26 (-5.3%)	101.16 (-6.4%)	98.23 (-9.1%)	98.02 (-9.3%)	92.67 (-14.2%)	92.37 (-14.5%)	90.88 (-15.9%)	86.14 (-20.3%)
	B (1800)	68.17 (0.0%)	62.06 (-9.0%)	67.93 (-0.3%)	55.78 (-18.2%)	60.82 (-10.8%)	55.76 (-18.2%)	58.25 (-14.5%)	62.48 (-8.3%)	63.21 (-7.3%)	59.13 (-13.3%)	62.42 (-8.4%)
	C (2400)	32.82 (0.0%)	30.70 (-6.5%)	31.04 (-5.4%)	31.67 (-3.5%)	33.61 (2.4%)	31.96 (-2.6%)	31.84 (-3.0%)	34.76 (5.9%)	31.61 (-3.7%)	35.47 (8.1%)	37.52 (14.3%)
	D (3500)	17.91 (0.0%)	18.71 (4.5%)	19.11 (6.7%)	19.07 (6.5%)	20.32 (13.5%)	19.46 (8.7%)	19.16 (7.0%)	19.76 (10.4%)	19.78 (10.4%)	20.78 (16.1%)	20.71 (15.7%)
	E (4400)	17.09 (0.0%)	17.07 (-0.1%)	17.14 (0.3%)	17.60 (3.0%)	17.16 (0.4%)	18.09 (5.8%)	18.06 (5.7%)	17.79 (4.1%)	17.87 (4.6%)	18.71 (9.5%)	18.60 (8.8%)

*Speed(kph)(ratio) Speed(kph)

Fig. 12. Travel speed patterns according to different LOS and MPR levels.

and investigated to improve the performance. One feasible alternative is the design of an artificial intelligence controller based on reinforcement learning, which the authors have been working on as a further study. Third, there should be an attempt to obtain the target speed to address multiple other objectives, including the operational efficiency and the environmental impacts, rather than just focusing on the safety. This is because these three objectives are fundamentally determined by individual vehicle maneuverings. Finally, more systematic simulation calibration and validation need to be conducted with a larger vehicle trajectory dataset. Various traffic conditions and vehicle types should also be taken into consideration in comparing the actual data and the simulated data.

Acknowledgement

This work was also supported by a grant from the National Research Foundation of Korea funded by the Korean government (MSIP) (NRF-2017R1A2B4005835).

References

Darbha, S., Rajagopal, K.R., 1999. Intelligent cruise control systems and traffic flow stability. Transp. Res. Part C Emerg. Technol. 7, 329–352.
Jeong, E., Oh, C., 2017. Evaluating the effectiveness of active vehicle safety systems. Accid. Anal. Prev. 100, 85–96.
Jeong, E., Oh, C., Lee, S., 2017. Is vehicle automation enough to prevent crashes? Role of traffic operations in automated driving environments for traffic safety. Accid. Anal. Prev. 104, 115–124.
Ji, J., Khajepour, A., Melek, W.W., Huang, Y., 2017. Path planning and tracking for vehicle collision avoidance based on model predictive control with multiconstraints. IEEE Trans. Veh. Technol. 66 (2), 952–964.
Jula, H., Kosmatopoulos, E.B., Ioannou, P.A., 2000. Collision avoidance analysis for lane changing and merging. IEEE Trans. Veh. Technol. 49 (6), 2295–2308.
Kim, K., Kim, B., Lee, K., Ko, B., Yi, K., 2017. Design of integrated risk management-based dynamic driving control of automated vehicles. IEEE Intell. Transp. Syst. Mag. 9 (1), 57–73.
Lee, S., Jeong, E., Oh, M., Oh, C., 2019. Driving aggressiveness management policy to enhance the performance of mixed traffic conditions in automated driving environments. Transp. Res. Part A Policy Pract. 121, 136–146.
Li, L., Wen, D., Yao, D., 2014. A survey of traffic control with vehicular communications. IEEE Trans. Intell. Transp. Syst. 15 (1), 425–432.
Pan, D., Zheng, Y., Qiu, J., Zhao, L., 2017. Synchronous control of vehicle following behavior and distance under the safe and efficient steady-following state: two case studies of high-speed train following control. IEEE Trans. Intell. Transp. Syst.
Park, H., Oh, C., Moon, J., 2018. Real-time estimation of lane change risks based on the analysis of individual vehicle interactions. Transp. Res. Rec. 2672 (20), 39–50.
Pueboobpaphan, R., Arem, B., 2011. Driver and vehicle characteristics and platoon and traffic flow stability. Transp. Res. Rec.: J. Transp. Res. Board 2189, 89–97. https://doi.org/10.3141/2189-10.
Schakel, W.J., Arem, B., Van Netten, B.D., 2010. Effects of cooperative adaptive cruise control on traffic flow stability. Intell. Transp. Syst. (ITSC) 2010 13th Int. IEEE Conf 759–764. https://doi.org/10.1109/ITSC.2010.5625133.
Schmidt, K., Beggiato, M., Hoffmann, K.H., Krems, J.F., 2014. A mathematical model for predicting lane changes using the steering wheel angle. J. Saf. Res. 49, 81–85.
Schubert, R., Schulze, K., Wanielik, G., 2010. Situation assessment for automatic lane-change maneuvers. IEEE Trans. Intell. Transp. Syst. 11 (3), 607–616.
Shiller, Z., Prasanna, R., Salinger, J., 2008. A Unified Approach to Forward and Lane Change Collision Warning for Driver Assistance and Situational Awareness. SAE Technical Paper.
Shrivastava, A., Li, P.Y., 2000. Traffic flow stability induced by constant time headway policy for adaptive cruise control (ACC) vehicles. Proc. 2000 Am. Control Conf. ACC (IEEE Cat. No.00CH36334) 3, 275–301.
Talebpour, A., Mahmassani, H., Hamdar, S., 2013. Speed harmonization: evaluation of effectiveness under congested conditions. Transp. Res. Rec.: J. Transp. Res. Board 2391, 69–79.
Wang, C., Stamatiadis, N., 2013. Surrogate safety measure for simulation-based conflict study. Transp. Res. Rec.: J. Transp. Res. Board 2386, 72–80.
Wang, C., Stamatiadis, N., 2014. Derivation of a new surrogate measure of crash severity. Transp. Res. Rec.: J. Transp. Res. Board 2432, 37–45.
Wang, M., Shan, H., Lu, R., Zhang, R., Shen, X., Bai, F., 2015. Real-time path planning based on hybrid-VANET-enhanced transportation system. IEEE Trans. Veh. Technol. 64 (5), 1664–1678.
Xiaorui, W., Hongxu, Y., 2013. A lane change model with the consideration of car following behavior. Procedia-Soc. Behav. Sci. 96, 2354–2361.